Journal of Fluorescence, Vol. 8, No. 1, 1998

Fluorescence Spectroscopy of Potential Electroluminescent Materials: Substituent Effects on DSB and Segmented PPV Derivatives

E. Birckner,[1] U.-W. Grummt,[1] H. Rost,[2] A. Hartmann,[2] S. Pfeiffer,[2] H. Tillmann,[2] and H.-H. Hörhold[2]

Received October 27, 1997; accepted February 27, 1998

The absorption and fluorescence of substituted distyrylbenzene (DSB) derivatives and segmented poly(phenylene vinylene) (PPV) derivatives are characterized by long-wavelength absorption maxima and absorption coefficients of λ_a = 380–450 nm, ε = 20,000–60,000 M^{-1} cm^{-1} and fluorescence maxima, quantum yields, and decay times of λ_f = 440–530 nm, Φ_f = 0.2–0.9, and τ = 0.8–2.5 ns, respectively. Alkoxy substituents at the central phenylene ring of DSB groups increase the bathochromic shift in the spectra in comparison to DSB, without a significant decrease in the high DSB fluorescence quantum yield. Both phenyl and cyano substitutions at the vinylene bridge lead to a further bathochromic shift of the fluorescence and a decrease in the quantum yield to ca. 0.4. The DSB derivatives and the related segmented PPV derivatives show nearly the same absorption spectra, fluorescence spectra, and radiative rate constants $k_f = \Phi_f/\tau$, indicating the efficacy of the segmentation of the polymer chain. The radiative rate constants determined by the Φ_f and τ values and by the Strickler/Berg formula are in reasonable agreement. This supports the possibility of interpreting the properties of the polymers in terms of their DSB units. The decrease in the emission anisotropy can be ascribed to multistep energy transfer processes between different oriented segments.

KEY WORDS: DSB derivatives; segmented PPV derivatives; substituent effects; fluorescence spectra; quantum yields; lifetimes; emission anisotropy; energy transfer.

INTRODUCTION

In the past years conjugated polymers such as poly(phenylene vinylene) (PPV) have attracted increasing interest as active materials for light emitting diodes [1]. Furthermore, for PPV derivatives the wide tuning range across the visible spectrum and the high photoluminescence quantum yield in both solution and films suggest the use of these materials as an active laser medium [2]. Recently, a number of segmented PPV derivatives, **1** and **2** (Scheme I), were synthesized and found to be highly fluorescent [3,4]. They can be used as light-emitting materials in efficient LEDs [4–6,14]. From this application aspect and the close coherence of photo- and electroluminescence, an intensive study of the luminescence behavior of these PPV derivatives is necessary.

Thus, in this presentation we report the fluorescence characterization (spectra, quantum yield, decay time, polarization) of polymers **1** and **2** and the low molecular distyrylbenzene (DSB) model compounds **3**. The photophysical properties of the compounds are discussed with respect to the steric and electronic effects of the substituents and the segmenting unit.

[1] Institute of Physical Chemistry, University Jena, Lessingstraße 10, D-07743 Jena, Germany.

[2] Institute of Organic Chemistry and Macromolecular Chemistry, University Jena, Humboldtstraße 10, D-07743 Jena, Germany.

1053-0509/98/0300-0073$15.00/0

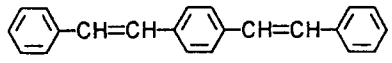

DSB

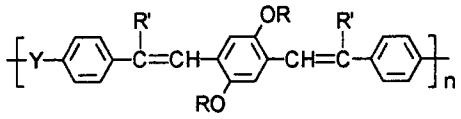

1 (R' = H) 2 (R' = Phenyl)

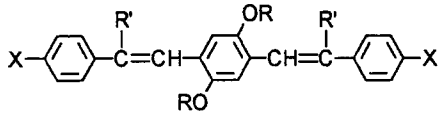

3 (R' = H , CN)

Scheme I

MATERIALS AND METHODS

Polymers **1** and **2** were prepared as described previously [3,4] by step growth polymerization through carbonylolefination reaction of dialdehydes or diketones using the Horner reaction and Wittig reaction, respectively. The polymers were characterized by gel permeation chromatography (PS standard) to have M_n = 6000–15,000 g/mol and M_w = 18,000–53,000 g/mol [4]. The DSB derivatives **3** are well characterized trans–trans isomers and were synthesized by Horner, Wittig, or Knoevenagel reaction using appropriate combinations of difunctional and monofunctional components [3,4,13–15]. The detailed synthesis and characterization of DSB derivatives **3** are given in the Appendix.

The solvent used for absorption and fluorescence measurements (dioxane) was of spectroscopic grade (Uvasol; Merck).

Absorption spectra were recorded with a Lambda 16 spectrophotometer (Perkin Elmer). Steady-state fluorescence and emission polarization measurements were performed with a LS-50B luminescence spectrometer (Perkin Elmer).

Fluorescence kinetics using nanosecond flashlamp excitation (H_2-gas filling; pulse width, 1.2 ns) were measured by means of the time-correlated single-photon counting method (time-resolved fluorescence spectrometer FL900CDT; Edinburgh Instruments). Polarizers with a vertical orientation on the excitation side and a 55° (magic angle) orientation on the emission side were used to avoid polarization effects.

Fluorescence quantum yields were determined from the integrated quantum-corrected fluorescence spectra of diluted solutions (absorbance, ≤0.05) relative to that of quinine sulfate (Fluka, puriss.) in 0.1 *N* H_2SO_4 (Φ_f = 0.55) and were corrected regarding the refractive index of the solvent with n^2.

To calculate fluorescence lifetimes from the decay curves the LEVEL 1 (up to four exponentials) and LEVEL 2 (global analysis and Förster-type analysis) packages implemented in the Edinburgh Instruments software were used. Plots of weighted residuals and of the autocorrelation function and values of reduced residuals χ^2 were used to judge the quality of the fit.

RESULTS AND DISCUSSION

The existence of different isomers and rotamers with different photophysical properties is principally expected for the newly synthesized compounds for structural reasons.

Cis–trans photoisomerization as well as spectra, quantum yields, and lifetimes of the EE, EZ, and ZZ isomers of DSB is reported in Ref. 7. To prevent errors in the experimental data due to photochemical reactions, we prepared and handled the samples in the dark. Absorption spectra measured before and after the fluorescence measurements showed only small or no differences.

Rotamerism of substituted diarylethylenes is reviewed in Ref. 8. This is manifested by the excitation wavelength dependence of fluorescence spectra, quantum yields, and lifetimes, especially at lower temperatures. We found no significant differences with our compounds between absorption spectra and fluorescence excitation spectra and no indications for distinguishable rotamers at room temperature.

The absorption and fluorescence of the substituted DSB and segmented PPV derivatives in dioxane solutions at room temperature are characterized by long-wavelength absorption maxima and absorption coefficients of λ_a = 380–450 nm and ε = 20,000–60,000 M^{-1} cm^{-1} and fluorescence maxima, quantum yields, and decay times of λ_f = 440–530 nm, Φ_f = 0.2–0.9, and τ = 0.8–2.5 ns, respectively (Table I).

The absorption and fluorescence spectra of the unsubstituted model compound DSB and of differently *R*- and *R'*-substituted DSB derivatives (DOO–DSB;**3f**) are given in Fig. 1. The spectra and the high absorption coefficient of DSB [9] indicate a planar, flexible struc-

Table I. Absorption Maxima (λ_a) and Molar Absorption Coefficients (as logε), Fluorescence Maxima (λ_f), Stokes Shifts ($\Delta\nu_{St}$), Quantum Yields (Φ_f), Lifetimes (τ), Mean Lifetimes ($\langle\tau\rangle$; See Text), and Anisotropies (r) of DSB and Segmented PPV Derivatives in Dioxane[a]

	Y	*R*	*R'*	λ_a (nm)	logε	λ_f (nm)	$\Delta\tilde{\nu}$ (cm^{-1})	Φ_f	$\langle\tau\rangle$ (ns)	*r*
1a	—	C_8H_{17}	H	425	4.30	482	2800	0.78	0.87	0.23
1b	O	C_8H_{17}	H	402	4.60	446	2450	0.82	1.20	0.067
1c	CHOH	C_8H_{17}	H	395	4.51	447	2900	0.87		
1d	CO	C_8H_{17}	H	425	4.60	486	3000	0.66	1.26	0.080
1e	NPh	C_8H_{17}	H	442	4.70	494	2400	0.66		
2a	—	CH_3	Ph	401	4.53	496	2000	0.72	1.47	0.046
2b	O	CH_3	Ph	390	4.46	490	5200	0.43	1.15	0.038
2e	NPh	CH_3	Ph	403	4.42	512	5300	0.28	0.83	0.089
	X									
DSB				355	4.80	388	2400	0.90	1.29	0.051
DOO–DSB	H	C_8H_{17}	H	387	4.48	440	3100	0.83	1.74	0.040
3a	Ph	C_8H_{17}	H	405	4.30	460	2950	0.90	1.35	0.12
3b	O–Ph	C_8H_{17}	H	392	4.63	444	3000	0.91	1.49	0.11
3c	CHOH–Ph	C_8H_{17}	H	388	4.51	445	3300	0.81		
3d	CO–Ph	C_8H_{17}	H	415	4.60	487	3560	0.70	1.52	0.12
3e	NPh_2	CH_3	H	425	4.82	480	2700	0.75	1.26	0.18
3f	H	C_8H_{17}	CN	425	4.36	512	4000	0.36	2.90	0.038
3g	O–Ph	C_8H_{17}	CN	433	4.47	512	3560	0.49	2.23	0.075

[a]Ph, phenyl.

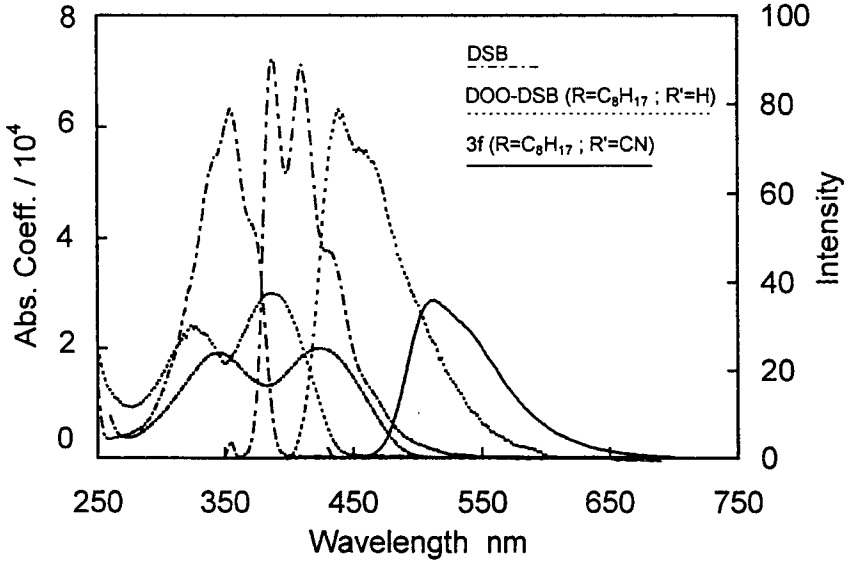

Fig. 1. Scheme Absorption and fluorescence spectra of DSB and of *R*- and *R'*-substituted DSB derivatives (DOO–DSB; **3f**) in dioxane.

ture in the S_0 ground state and a planar, but less flexible structure in the fluorescent S_1 state. The energy differences of ca. 1400 cm^{-1} of the shoulders in the absorption spectrum are related to those of the vibrational structure in the fluorescence spectrum and are typical for many aromatic hydrocarbons. They are assigned to C–C vibrational modes. The long-wavelength electron transition is dipole allowed ($\pi\pi^*$) and it is oriented essentially parallel to the long molecular axis [10].

Substitution of DSB at the vinylene groups with bulky phenyl substituents (not included in Table I) shows the effect of the deviation from planarity in the

Table II. Fluorescence Rate Constants, Determined by $k_f = \Phi_f/\tau$ and by the Strickler/Berg Formula [k_f(SB)] and Rate Constants $k_{nr} = (1 - \Phi_f)/\tau$ of Radiationless Deactivation

	Φ_f/τ (10^8 s^{-1})	k_f (SB) (10^8 s^{-1})	k_{nr} (10^8 s^{-1})
1a	0.90	0.17	0.25
1b	0.68	0.38	0.15
1d	0.52	0.34	0.27
2a	0.49	0.26	0.19
2b	0.37	0.21	0.50
2e	0.34	0.25	0.87
DSB	0.70	0.84	0.077
DOO–DSB	0.48	0.26	0.098
3a	0.67	0.43	0.074
3b	0.61	0.40	0.060
3d	0.46	0.37	0.20
3e	0.60	0.52	0.20
3f	0.12	0.13	0.22
3g	0.22	0.19	0.23

equilibrated ground and excited state on the absorption and fluorescence: in comparison to DSB the molar absorption coefficient and the fluorescence quantum yield are reduced (log ε = 4.48, Φ_f = 0.06), and the fluorescence spectrum is unstructured and strongly redshifted ($\delta\ \nu_{St}$ = 6860 cm^{-1}).

Alkoxy substituents at the central phenylene ring of DSB groups blur the vibrational structure and increase the bathochromic shift in both the absorption and the fluorescence spectra in comparison to DSB, without a decrease in the DSB fluorescence quantum yield. The buildup of a second, less intense absorption band (electronic transition) in the region from 300 to 350 nm is typical for all alkoxy-substituted compounds under investigation.

Substitution at the vinylene bridge (R' = CN or Ph) in addition to alkoxy substitution leads to a further bathochromic fluorescence shift. The fluorescence quantum yield is reduced to ca. 40%.

The radiative rate constants $k_f = \Phi_f/\tau$ for the compounds unsubstituted in the R' position are high, as expected for dipole-allowed transitions, but reduced in the derivatives R' = CN (**3f, 3g**). The k_f values determined by Φ_f and τ and by the Strickler/Berg formula (k_f(SB) [11]) are generally in good agreement (Table II). The larger $k_f = \Phi_f/\tau$ values of DOO–DSB, **3a, 3b**, and **3d** indicate a more planar geometry in the S_1 than in the S_0 state.

The DSB derivatives with X = CHOH–Ph, O–Ph, and CO–Ph and the related PPV derivatives with Y = CHOH, O, and CO (Scheme I) show nearly the same absorption spectra, fluorescence spectra, and radiative rate constants $k_f = \Phi_f/\tau$, indicating the efficacy of the segmentation of the polymer chain by these Y groups (Fig. 2, Tables I and II). The radiative rate constants determined by the Φ_f and τ values and by the Strickler/Berg formula are in reasonable agreement. This supports the possibility of interpreting the properties of the polymers in terms of their DSB units.

Larger differences in the spectra of the DSB derivatives and the related PPV derivatives are measured with Y = NPh as the segmentation unit. Obviously, the con-

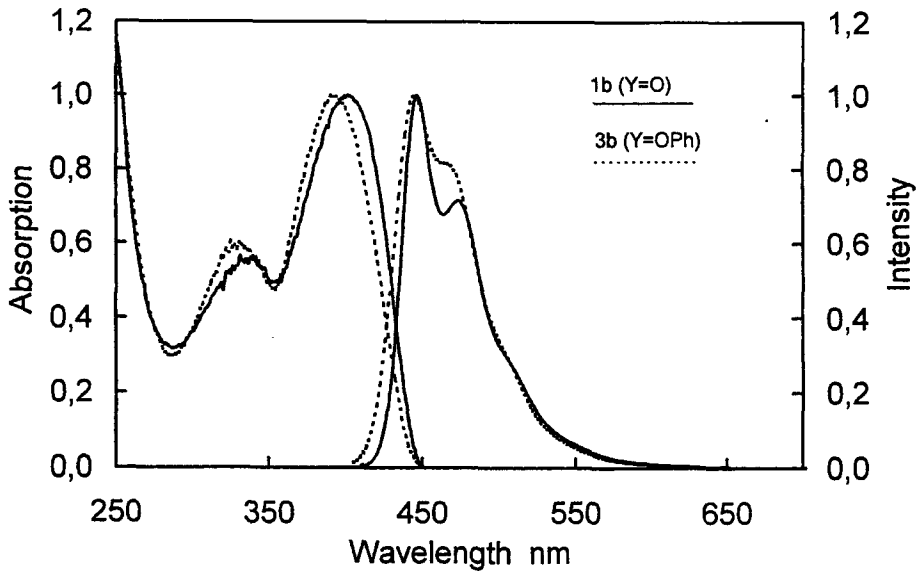

Fig. 2. Absorption and fluorescence spectra of PPV (**1b**) and related DSB (**3b**) derivatives in dioxane.

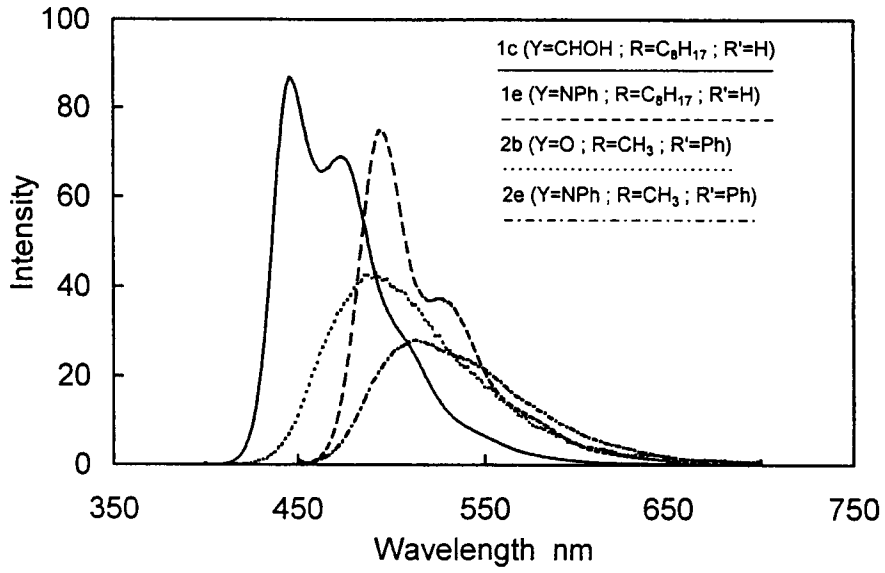

Fig. 3. Fluorescence spectra of *R'*-substituted (**2b**, **2e**) and *R'*-unsubstituted (**1c**, **1e**) PPV derivatives in dioxane.

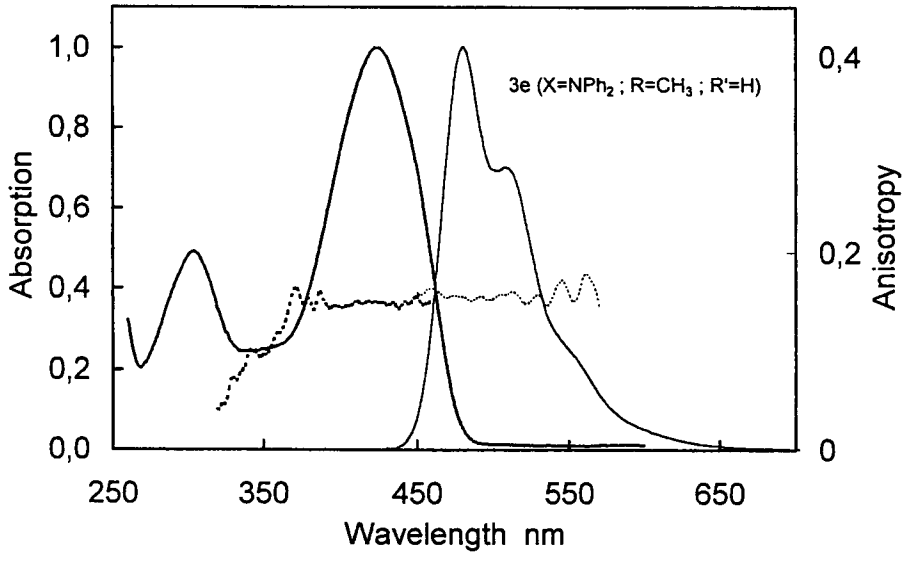

Fig. 4. Absorption and fluorescence spectra and excitation and emission anisotropy spectra of the DSB derivative **3e** in dioxane.

jugation along the PPV chain is extended over more than 1 DSB unit.

The fluorescence spectra of the *R'*-substituted PPV derivatives are unstructured due to the less planar geometry in the excited state in comparison to the unsubstituted compounds (Fig. 3).

The fluorescence kinetics of the DSB derivatives is essentially single exponential. The reason for the small deviations from a single-exponential decay could be due to emission of rotamers with different lifetimes and is to be clarified by further investigations.

The kinetics of the polymers is nonexponential. Although it fits Förster-type kinetics rather than a biexponential model, the data in Table I are given as mean lifetimes $\langle\tau\rangle$ from biexponential calculations to avoid misinterpretations. Förster-type kinetics with a decay function given by $I(t)=I_0*\exp\,[(-t/\tau)-2\gamma*\sqrt{(t/\tau)}]$ is valid only for the kinetics of the donor fluorescence in

a donor–acceptor energy transfer process. In our case we have to assume the superposition of donor and acceptor fluorescence additionally to possible rotamer emissions.

The mean lifetimes of the polymers are shortened in comparison to those of the related DSBs, due mainly to an increase in the nonradiative deactivation, k_{nr} (Table II).

The fluorescence anisotropy of all compounds is also nonzero in the low-viscosity solvent dioxane due to the rod-like shape of the molecules, the orientation of the transition moments parallel to the long molecule axis, and the short fluorescence lifetime. The effective rotation volume, calculated from the emission anisotropies and lifetimes using the Stokes–Einstein equation, are in good agreement with the molecular dimensions of the DSB derivatives.

In the case of the polymers with absorbing and emitting segments, which do not rotate perpendicularly to the transition moments, the emission anisotropy should be maximal, i.e., ≈0.4. The decrease in emission anisotropy can be ascribed to multistep energy transfer processes between differently oriented segments.

The rate of energy transfer for **1b** between two neighboring segments was calculated by the Förster formula [12] from the absorption and fluorescence spectra of **3b** and the angle and distance between two neighboring segments. It is of the order of 10^{11} s^{-1} and ca. 100 times larger than the transfer rate to the second neighboring segment.

The high anisotropy of 0.23 for **1a** is due to the nearly linear alignment of neighboring segments (angle between the transitions moments ≈0°) in the polymer chain, i.e., energy transfer in this PPV derivative is not connected with strong depolarization.

APPENDIX: PREPARATION AND CHARACTERIZATION OF DSB MODEL COMPOUNDS

DSB: Distyrylbenzene

DSB was prepared and characterized according to Ref. 13. T_m, 265°C.

DOO–DSB: 1,4-Bis(styryl)-2,5-dioctyloxybenzene (trans–trans) [14]

2,5-Dioctyloxy-1,4-xylylene-bis(diethylphosphonate) (4.1 g, 6 mmol) and benzaldehyde (1.4 g, 13 mmol) were dissolved under argon in 150 ml toluene and heated under stirring to 80°C. To this solution, solid potassium-t-butylate (1.45 g, 13 mmol) was added in one portion. After 2 h at reflux the reaction mixture was quenched with 100 ml of aqueous acetic acid. The organic layer was then seperated, washed several times with distilled water, and dried. The solvent was reduced to a minimum and the residue was purified by column chromatography (aluminum oxide, toluene). The yellow solution was then evaporated to dryness to give brilliant yellow crystals (2.0 g; 58%). T_m (DSC): 108°C. FTIR (KBr): γ(CH) 962 (*trans*-vinylene).

$C_{38}H_{50}O_2$ (538.7). Calc.: C 84. 70; H, 9.35. Found: C, 84.62; H, 9.33.

^{13}C NMR (CD_2CL_2) δ/ppm: 151.5, 138.3, 132.4, 129.0, 127.8, 127.2, 126.8, 123.7, 110.9, 69.9, 32.2, 29.9, 29.8, 29.6, 26.7, 23.0. ^1H NMR (CD_2Cl_2) δ/ppm: 7.6–7.0 (m, 16 H); 4.1–4.0 (t, 4 H); 1.8–1.2 (m, 24 H); 0.8 (t, 6H).

3b: 1,4-Bis(4-phenoxystyryl)-2,5-dioctyloxybenzene (trans–trans) [4]

2,5-Dioctyloxy-1,4-xylylene-bis(diethylphosphonate) and 4-phenoxy-benzaldehyde were reacted analogously. The solution of the chromatographed product was evaporated to dryness to give brilliant yellow crystals (yield, 92%). T_m (DSC): 92°C. FTIR (KBr)ν/cm^{-1}: γ(CH) 967 (*trans*-vinylene).

$C_{50}H_{58}O_4$ (722.9). Calc.: C, 83.07; H, 8.08. Found: C, 82.23; H, 8.10.

^{13}C NMR ($CDCl_3$) δ/ppm: 157.2, 151.4, 133.7, 130.1, 128.1, 127.1, 126.9, 123.7, 122.9, 119.3, 110.8, 70.0, 32.2, 29.9, 29.8, 29.7, 26.7, 23.1, 14.3. ^1H NMR ($CDCl_3$) δ/ppm: 7.55–7.06 (m, 24H); 4.09–4.00 (t, 4H); 1.94–1.31 (m, 24H); 0.91–0.86 (t, 6H).

3c: 1,4-Bis[4-(phenyl-hydroxymethyl)styryl]-2,5-dioctyloxybenzene (trans–trans)

2,5-Dioctyloxy-1,4-bis(4-benzoyl-styryl)benzene (1.2 g, 1.6 mmol) was dissolved in 100 ml toluene/ethanol (10:1) under stirring to 70°C. $NaBH_4$ (1.2 g, 32 mmol) was added carefully in portions, and after 2 h of stirring at 50°C the mixture was quenched with 100 ml of aqueous acetic acid. The organic layer was then seperated, washed several times with distilled water, and dried with Na_2SO_4. The solvent was reduced to a minimum and the residue was purified by column chromatography (aluminum oxide, toluene). The eluent was removed to give yellow crystals (1.12 g; 93%). T_m (DSC): 81°C. FTIR (KBr) ν/cm^{-1}: ν(OH) 3326, γ(CH) 969 (*trans*-vinylene).

$C_{52}H_{62}O_4$ (750.9). Calc.: C, 83.16; H, 8.32. Found: C, 82,66; H, 8.80.

^{13}C NMR ($CDCl_3$) δ/ppm: 151.4, 144.5, 143.8, 137.6, 128.8, 128.5, 127.8, 127.1, 127.0, 126.9, 126.7, 123.7, 110.7, 76.2, 69.9, 32.2, 30.1, 29.8, 29.7, 26.6, 23.1, 14.3.

3d: 1,4-Bis(4-benzoyl-styryl)-2,5-dioctyloxybenzene (trans–trans)

2,5-Dioctyloxyterephthalaldehyde (3.9 g, 10 mmol) and 4-benzoyl-benzyltriphenylphosphoniumbromide (10.7 g, 20 mmol) were dissolved under argon in 200 ml DMF and heated under stirring to 70°C. To this solution, solid potassium-t-butylate (3.4 g, 30 mmol) was added in one portion. After 2 h of stirring at 50–60°C, the reaction mixture was quenched with 200 ml of aqueous acetic acid. The precipitate was filtered off and the filtrate extracted a few times with toluene. Precipitate and extract were combined and dried over Na_2SO_4. The solvent was reduced to a minimum and the residue was purified by column chromatography (aluminum oxide, toluene). The eluent was removed to give an orange solid (4.33 g, 58%). T_m (DSC): 127°C. FTIR (KBr) ν/cm^{-1}: ν(C=O) 1653, γ(CH) 960 (*trans*-vinylene).

$C_{52}H_{58}O_4$ (746.9). Calc.: C, 83.61; H, 7.83 Found: C, 82.97; H, 8.00.

3e: 1,4-Bis(4-diphenylamino-styryl)-2,5-dimethoxybenzene (trans–trans) [4]

2,5-Dimethoxy-1,4-xylylene-bis(diethylphosphonate) (2.20 g, 5 mmol) and 4-formyltriphenylamine (3.30 g, 12 mmol) were dissolved under argon in 40 ml toluene and heated under stirring to 80°C. To this solution solid potassium-t-butylate (2.25 g, 20 mmol) was added in one portion. After 2 h at reflux the reaction mixture was quenched with 20 ml of aqueous acetic acid. The organic layer was then separated, washed several times with distilled water, and dried with Na_2SO_4. The solvent was removed and the residue recrystallized from toluene to give yellow crystals (2.56 g, 78%). T_m (DSC): 236°C. FTIR (KBr) ν/cm^{-1}: γ(CH) 967 (*trans*-vinylene).

$C_{48}H_{40}N_2O_2$ (676,8). Calc.: C, 85.21; H, 5.92; N, 4.14. Found: C, 82.54; H, 5.91; N, 4.07.

^{13}C NMR ($CDCl_3$) δ/ppm: 151.5, 147.6, 147.2, 132.2, 129.3, 128.3, 127.8, 127.4, 126.6, 124.4, 123.7, 123.0, 109.0, 56.4. ^1H NMR ($CDCl_3$) δ/ppm: 7.5–7.0 (m, 34 H); 3.9 (s, 6 H).

3f: 1,4-Bis(β-cyano-styryl)-2,5-dioctyloxybenzene (trans–trans) [15]

A mixture of 2,5-dioctyloxyterephthalaldehyde (5 mmol) and benzeneacetonitrile (12.5 mmol) in 50 ml ethanol (50 ml) was refluxed under argon until dissolution was complete. Potassium t-butylate (solution of 60 mg in 0.5 ml t-butanol) was added, and the mixture was stirred under reflux for 1 h. After neutralization with acetic acid and cooling to room temperature, the crystalline product precipitated, was washed with water/methanol, and recrystallized from acetone to give orange crystals (yield, 70%). T_m = 125°C. FTIR (KBr): ν(C–N) 2211.

$C_{40}H_{48}N_2O_2$ (588.4). Calc.: C, 81.63; H, 8.16; N, 4.76. Found: C, 82,30; H, 8.18; N, 4.65.

^{13}C NMR ($CDCl_3$) δ/ppm: 151.5, 136.1, 134.7, 129.2, 129.1, 126.1, 125.8, 118.3, 111.8, 111.4, 69.5, 31.7, 29.3, 29.3, 29.2, 26.2, 22.6, 14.1. ^1H NMR ($CDCl_3$) δ/ppm: 8.02 (s, 2H); 7.88 (s, 2H); 7.70–7.67 (d, 4H); 7.48–7.36 (m, 6H); 4.13–4.08 (t, 4H); 1.89–1.23 (m, 24H); 0.87–0.82 (t, 6H).

3g: 1,4-Bis(4-phenoxy-β-cyano-styryl)-2,5-dioctyloxybenzene (trans–trans) [15]

2,5-Dioctyloxyterephthalaldehyde and 4-phenoxybenzeneacetonitrile were reacted analogously. The product was recrystallized from acetone to give red needles (yield, 78%). T_m = 108°C. FTIR (KBr) ν/cm^{-1}: ν(C–N) 2211.

$C_{52}H_{56}N_2O_4$ (772.5). Calc.: C, 80.84; H, 7.25; N, 3.62 Found: C, 80.28; H, 7.46; N, 3.70.

^{13}C NMR ($CDCl_3$) δ/ppm: 158.6, 156.2, 151.4, 134.9, 129.9, 129.4, 127.6, 125.7, 124.1, 119.6, 118.7, 118.4, 111.2, 111.0, 69.4, 31.7, 29.3, 29.3, 29.2, 26.2, 22.6, 14.1. ^1H NMR ($CDCl_3$) δ/ppm: 7.93 (s, 2H); 7.85 (s, 2H); 7.65–7.61 (d, 4H); 7.39–7.34 (2d, 4H); 7.17–7.13 (t, 2H); 7.06–7.03 (m, 8H); 4.11–4.08 (t, 4H); 1.84–1.24 (m, 24H); 0.85–0.81 (t, 6H).

ACKNOWLEDGMENT

The authors gratefully thank the BMBF (03N 1004E1) and SFB 196 (DFG) for support.

REFERENCES

1. J. H. Burroughes, D. D. C. Bradley, A. R. Brown, R. N. Marks, K. MacKay, R. H. Friend, P. L. Burn, and A. B. Holmes (1990) *Nature* **347**, 539. D. Brown and A. J. Heeger (1991) *Appl. Phys.*

Lett. **58**, 1982. J. R. Sheats, H. Antoniadis, M. Hueschen, W. Leonard, J. Miller, R. Moon, D. Roitman, and A. Stocking (1996) *Science* **273**, 884.
2. D. Moses (1992) *Appl. Phys. Lett.* **60**, 12215. F. Hide, B. Schwartz, M. A. Diaz-Garcia, and A. J. Heeger (1996) *Chem. Phys. Lett.* **256**, 424.
3. H. Rost, S. Pfeiffer, A. Teuschel, and H.-H. and Hörhold (1997) *Synth. Metals* **84**, 269.
4. H.-H. Hörhold, H. Rost, A. Teuschel, W. Kreuder, and H. Spreitzer (1998) *Proc. SPIE* **3148**, in press.
5. W. Kreuder, D. Lupo, J. Salbeck, H. Schenk, T. Stehlin, H.-H. Hörhold, A. Lux, A. Teuschel, and M. Wieduwilt (1996) WO 96/10617, Hoechst AG.
6. W. Kreuder, H.-H. Hörhold, and H. Rost (1997) DE 19532574A1 (OS 6.3.1997), Hoechst AG.
7. K. Sandros, M. Sundahl, O. Wennerstrom, and U. Norinder (1990) *J. Am. Chem. Soc.* **112**, 3082–3086.
8. U. Mazzucato and F. Momicchioli (1991) *Chem. Rev.* **91**, 1679–1719.
9. R. Erckel and H. Frühbeis (1982) *Z. Naturforsch* **37b**, 1472–1480.
10. K. Gustav and A. Geyer (1992) *J. Prakt. Chem.* **334**, 505–508.
11. S. J. Strickler and R. A. Berg (1962) *J. Chem. Phys.* **37**, 814.
12. Th. Förster (1948) *Ann. Phys.* **2**, 55.
13. G. Drefahl, R. Kühmstedt, H. Oswald, and H.-H. Hörhold (1970) *Makromol. Chem.* **131**, 89
14. H. Rost, H.-H. Hörhold, W. Kreuder, and H. Spreitzer (1998) *Proc. SPIE* **3148**, in press
15. H. Tillmann and H.-H. Hörhold (1997) Poster presented at PAT '97, Polymers for Advanced Technology, Leipzig, Germany, Sept.